Archives Italiennes de Biologie, 147: 11-20, 2009.

Does the default-mode functional connectivity of the brain correlate with working-memory performances?

F. ESPOSITO[1,2], A. ARAGRI[3,4], V. LATORRE[3,5], T. POPOLIZIO[3], T. SCARABINO[3], S. CIRILLO[4,6], E. MARCIANO[1], G. TEDESCHI[4,6], F. DI SALLE[2,3,7]

[1] Department of Neuroscience, University of Naples "Federico II", Naples, Italy;
[2] Department of Cognitive Neuroscience, Maastricht University, Maastricht, The Netherlands;
[3] Unit of Neuroradiology, I.R.C.S.S. "Casa Sollievo della Sofferenza", S. G. Rotondo, Italy;
[4] Department of Neurological Sciences, Second University of Naples, Naples, Italy;
[5] Department of Psychiatry, University of Bari, Italy; [6] I.D.C. Hermitage Capodimonte, Naples, Italy;
[7] Department of Neurosciences, University of Pisa, Italy

ABSTRACT

The "default-mode" network is an ensemble of cortical regions that are typically deactivated during demanding cognitive tasks in functional magnetic resonance imaging (fMRI) studies. Using functional connectivity analysis, this network can be studied as a "stand-alone" brain system whose functional role is supposed to consist in the dynamic control of intrinsic processing activities like attention focusing and task-unrelated thought generation and suppression. Independent component analysis (ICA) is the method of choice for generating a statistical image of the "default-mode" network (DMN) using a task- and seed-independent distributed model of fMRI functional connectivity without prior specification of node region extent and timing of neural activation. We used a standard graded working-memory task (n-back) to induce fMRI changes in the default-mode regions and ICA to evaluate to DMN functional connectivity in nineteen healthy volunteers. Based on the known spatial variability of the ICA-DMN maps with the task difficulty levels, we hypothesized the ICA-DMN may also correlate with the subject performances. We confirmed that the relative extent of the anterior and posterior midline spots within the DMN were oppositely (resp. positively in the anterior and negatively in the posterior cingulate cortex) correlated with the level of task difficulty and found out that the spatial distribution of DMN also correlates with the individual task performances. We conclude that the working-memory function is related to a spatial re-configuration of the DMN functional connectivity, and that the relative involvement of the cingulate regions within the DMN might function as a novel predictor of the working-memory efficiency.

Key words

Functional magnetic resonance imaging; fMRI • Default-mode network • Working memory • Independent component analysis • Group-level analysis • Cognitive performance

Introduction

The "default-mode" network (DMN) is an ensemble of cortical regions that are deactivated during many different types of cognitive tasks (Rombouts et al., 2005a; Raichle and Snyder, 2007) and functionally coupled during rest (Greicius et al., 2003). Independently of the sensori-motor or cognitive status of the subject, the DMN is normally characterized by the functional coupling (functional connectivity) of several brain regions. DMN regions are normally located in the posterior cingulate cortex (PCC), medial prefrontal cortex (MPFC), which includes the perigenual anterior cingulate cortex

Corresponding Author: Fabrizio Esposito, c/o Unità di Audiologia e Vestibologia, II Policlinico (Nuovo Policlinico) Padiglione 13, via S. Pansini 5, 80131 Naples, Italy – Tel.: +39 081 7462883 - Fax: +39 081 7463581 - E-mail: fabrizio.esposito@unina.it

(ACC), lateral infero-parietal and infero-temporal cortices (Greicius et al., 2003). Hippocampus is also reported in some studies (see, e.g. Rombouts et al., 2003; Esposito et al., 2006, 2008) as co-activated to the other DMN regions.

The concept of a default-mode function has been originally introduced by Raichle and Snyder (2007) in an express attempt to differentiate a "cognitive" baseline state from a more "general" baseline state, coincident with the "resting" state of the human brain (but see also Mazoyer et al., 2001). Although this concept is currently still debated (see, e.g., Morcom and Fletcher, 2007), there have been successful attempts to link the mechanisms underlying the spatio-temporal modulation of the DMN regions to "implicit" brain processing functionalities and neural activity, such as focused attention (Fox et al., 2005) and task-unrelated thoughts (Fransson, 2006; Mason et al., 2007), as opposed to brain activity evoked by "explicit" cognitive tasks.

In the last few years, the functional connectivity of the two midline DMN regions along the cingulate cortex (MPFC and PCC) has been targeted as one cognitively relevant feature of the DMN pattern (see, e.g., Hampson et al., 2006; Sorg et al., 2007; Esposito et al., 2008), and most studies have converged towards a notion that DMN activity and connectivity is not just "disengaged" during cognitive tasks, but rather contributes to facilitating or monitoring cognitive performances. For instance, Hampson et al. (2006) initiated and supported that individual differences in the functional coupling between these two regions at rest would be able to predict differences in cognitive abilities, important for working memory task. Esposito et al. (2006) have highlighted that the entire spatial distribution of the DMN functional connectivity is modulated by the amount of working-memory engagement when the subject's cognitive status is changed by alternating periods of rest with periods of working-memory performance.

In functional magnetic resonance imaging (fMRI), the functional connectivity is assessed in terms of the linear correlations of blood oxygen level dependent (BOLD) time course data between two or more spatially remote regions. Seed-based (Biswal et al., 1997, 2005; Cordes et al., 2000) or clustering (Baumgartner et al., 1998; Goutte et al., 1999) techniques have been used for this purpose but independent component analysis (ICA, Hyvarinen et al., 2001) in its "spatial" variant (Calhoun et al., 2001; McKeown et al., 2003) is nowadays the most popular method for extracting multiple distributed functional connectivity patterns of neural activity from whole-brain fMRI time-series without prior specification of a temporal profile or spatial layout for the BOLD responses or any specific region as "seed" for the pattern statistical characterization.

Spatial ICA has been shown to reliably extract a statistical image of the "default-mode" network in single subjects and groups, under diverse fMRI experimental settings, ranging from resting-state experiments (Greicius et al., 2004b; van de Ven et al., 2004; Damoiseaux et al., 2006; Esposito et al., 2008) and simple sensory-motor tasks (Greicius et al., 2004a) up to cognitive tasks (Esposito et al., 2006) and free viewing naturalistic scenarios (Bartels and Zeki, 2005). More importantly, the individual variability of the spatio-temporal properties of the ICA-generated DMN patterns has been recently used in population studies for exploring possible correlations of DMN functional connectivity with cognitive decline (Greicius et al., 2004b; Rombouts et al., 2005a, 2005b; Sorg et al., 2007) and normal aging (Damoiseaux et al., 2008; Esposito et al., 2008; Sambataro et al., in press).

Hampson et al. (2006) have assessed the functional connectivity between PCC and MPFC in each subject using both seed-based and direct region-to-region correlation analyses starting from pre-defined regions-of-interest. In this study, separate periods of rest and working-memory tasks were compared for the strength of functional connectivity and the correlations with the task performances were estimated. One limitation of this study was that either one (the seed) or all DMN nodes had to be fixed in advance, with the consequence that the spatial distribution of the DMN functional connectivity could not be freely evaluated. On the other hand, we have previously demonstrated using ICA that DMN spatial distribution cannot be thought as invariant, thereby posing one operational difficulty of seed-based techniques in DMN functional connectivity analysis. In fact, the recruitment of the cingulate regions within the DMN network can significantly vary depending on the "average" cognitive status of the subject, and this distribution turns out to be correlated with the cognitive load (greater extension of the anterior and lesser

extension of the posterior cingulate cortices) when the subject alternates between lower and higher working memory loads (Esposito et al., 2006).

One limitation of our previous study (Esposito et al., 2006) is that only the objective difficulty of the task (i.e. 1- and 2-back in a standard n-back working-memory experiment) was considered as a factor, but not a more "implicit" or "subjective" factor, such as the individual working-memory performance (Pecini et al., 2008).

In the present study, we postulated that if this analytical information about the individual behavioural performances was taken into account, it may become possible to directly correlate the DMN network spatial distribution with how efficiently the working-memory function is actually operating. Compared to our previous study, the present one uses similar ICA methodology for extracting the DMN network maps, but applies it to a substantially extended sample of subjects and aims at correlating the size of the individual DMN regions of interests not only with the task difficulty but also with the task performance, as quantified by the average accuracy in the n-back task. The n-back experimental paradigm employs a sequence of objects presented with delays and allows stimulating the executive and maintenance functions of the working-memory (Gevins et al., 1993; Callicott et al., 1998; Jansma et al., 2000; Owen et al., 2005; Ciesielski et al., 2006; Bonino et al., 2008), while producing a sustained deactivation of the default-mode regions (McKiernan et al., 2003; Esposito et al., 2006). Here we explicitly aimed at investigating whether a correlation could be found out between the average accuracy in the task and the DMN functional connectivity distribution. This notion may potentially gather fundamental insight on the existence of delicate mechanisms of interplay between explicit (executive) and implicit (default) mechanisms of brain processing.

Methods

Subject and Experimental protocol

19 healthy subjects (5 males, mean age 28 ± 5, handedness (Edinburgh Inventory) 0.86 ± 0.18) performed the N-Back task as described in earlier reports (Bertolino et al., 2004). "N-back" refers to how far back in a sequence of stimuli the subject has to recall. The stimuli consisted of numbers (1-4) shown in random sequence and displayed at the points of a diamond-shaped box. There was a non-memory guided control condition (0-Back) that presented the same stimuli, but simply required subjects to identify the stimulus currently seen. The working memory task required recollection of a stimulus seen one stimulus (1-Back) or two stimuli (2-Back) previously while continuing to encode additionally incoming stimuli. Performance data were recorded as the number of correct responses (accuracy).

During the functional scans the stimuli were timed according to a block-design in which each block consisted of 15 scans (30s) of alternated rest and 0-back conditions for one run and 0-Back and N-Back (N = 1 or N = 2) for the other two runs. The order of runs was counterbalanced across subjects. The present study was approved by the local ethical board and all the subjects gave their informed consent in a written form.

MRI image data acquisition, preprocessing and visualization

Each subject was scanned using a GE Signa 3T scanner (Milwaukee, WI). Three time-series of 120 repeated gradient-echo EPI whole-brain images (TE = 30 msec, TR = 2 seconds, 20 contiguous slices, voxel dimensions = 3.75 x 3.75 x 5 mm) were acquired as fMRI BOLD data. After functional scans, co-registered 2D anatomical slices and 3D whole-head T1-weighted isometric (1 mm3) scans were acquired for correct 2D-3D registration and isotropic image time-series 3D resampling.

Functional image time-series were first corrected for the differences in slice acquisition times using a "sinc" interpolation technique, then, realigned with T1-volumes, warped into the standard anatomical space of Talairach and Tournoux (1988) and finally resampled to 3 x 3 x 3 mm^3 isotropic voxels. The Talairach transformation was performed in two steps. The first step consisted in rotating the 3-D data-set of each subject to be aligned with stereotaxic axes (for this step the location of the anterior commissure (AC), the posterior commissure (PC) and two rotation parameters for midsagittal alignment were specified manually). In the second step the extreme points of the cerebrum were specified. These points together with the AC and PC coordinates were, then, used to scale the 3-D data-sets into

the dimensions of the standard brain of the Talairach and Tournoux atlas using a piecewise affine and continuous transformation for each of the 12 defined subvolumes. The resulting voxel-time were filtered in time and space: low-frequency (drift) fluctuations were reduced using a high-pass temporal filter (3 cycles); spatial smoothing was performed using a 6 mm full-width at half-maximum gaussian kernel. For display purposes on the volumetric anatomy, individual maps were projected on the average volumetric image. Volumes with significant effects after thresholding of the group-level random-effects maps ($z = 3.1$, $p < 0.001$) were also segmented and rendered as surface meshes for three-dimensional views of the whole-brain distributed patterns.

All image data preparation and preprocessing steps as well as the map volumetric rendering were performed in BrainVoyager QX (www.brainvoyager.com, Brain Innovation, Maastricht, The Netherlands).

ICA and DMN functional connectivity analysis

We performed individual ICA and self-organizing group-level ICA (Sog-ICA, Esposito et al., 2005) of the pre-processed functional time-series using BrainVoyager QX plugins. Sog-ICA was performed separately for each session.

Prior to the ICA decomposition, the initial dimensions of the functional dataset were reduced to 25 using Principal Component Analysis. Then, an equal number of spatially independent components were estimated using the fastICA algorithm. The final number of dimensions kept at the PCA stage was chosen after an ICA reliability analysis (Himberg et al., 2004) performed on each subject data-set using the ICASSO Matlab package (www.mathworks.com). Using this tool we observed that using more than 25 dimensions did not produce more reliable components in any of the subjects' data sets. For each subject and session, the individual component time-courses of activity were parametrically correlated with the stimulus function, consisting of a box-car waveform with OFF and ON blocks of 15 time-points repeated 4 times in alternation, convolved with the standard double gamma hemodynamic response function (Friston et al., 1998).

Sog-ICA was used to group independent components by "clustering" the individual spatial patterns in the subject space. Cluster "group" components were calculated as random effects maps. Component clusters of interest were identified according to the intrinsic ranking in the hierarchical clustering and spatial matching to anatomical templates similar to previous related studies (Grecius et al., 2004b; Esposito et al., 2006). The spatial template-matching procedure consisted in comparing talairach coordinates of the centres-of-mass of each region in the group maps to those reported in previous studies. Following this approach, we identified the DMN components and applied a voxel-level threshold of $z = 3.1$ ($p < 0.001$, uncorrected) to the group random-effects map to identify DMN regions.

Starting from the DMN group ICA map of each session, we selected two volumes of interest (VOI), corresponding to the midline (MPFC and PCC) regions. These regions were quantified for all three sessions of the n-back experiment in term of the percentage of suprathreshold voxels (number of correlated voxels in the VOI x 100 / total number of correlated voxels in the spatial component). Then, we used these VOIs as masks to identify corresponding regions in the DMN of each subject and calculated similarly the correlated voxels percentages. These rates were collected from all subjects and sessions and were entered an analysis of covariance (ANCOVA) with two factors: one categorical factor (represented by the task difficulty with three levels, 0, 1 or 2, called "N-back") and one continuous factor (represented by the individual task performance accuracy, "Performance"). The performance accuracy was calculated for every subject in the n-back sessions by dividing the number of exact responses to the normalized overall number of presented stimuli (i.e.: ratio of the number of correct responses to the number of detectable responses). A linear correlation analysis between the individual rates of active voxels and the task performance accuracy was also performed for each separate session.

Results

The n-back performances were significantly different in the three sessions of the n-back task (mean values ± standard deviation: 2-back 77.78 ± 13.37, 1-back 97.97 ± 2.98 and 0-back 99.21 ± 1.53). We excluded two subjects from the analysis because

their performances for the 2-back sessions were below 50% (i.e. more than 1.5 times below the group standard deviation) and their after-session reports suggested a reduced cooperation or ability in performing the task.

ICA analyses of n-back time-series produced "default mode" components for each subject and n-back session. The individual DMN component time-courses were parametrically correlated with the stimulus function (the estimated absolute linear correlation coefficients, mean ± std, were 0.2803 ± 0.1671 for the 0-back session, 0.4833 ± 0.2063 for the 1-back and 0.6124 ± 0.1763 for the 2-back session).

For each session, the group-level DMN component was ranked high with respect to the subject-level spatial similarity in all three sessions. Although changes in the size of the constituent regions were observed (see below), all DMN components from the separate n-back sessions presented the same distributed architecture.

The spatial layout of the group-level ICA DMN maps for all three conditions were highly overlapping with the maps obtained in previous studies (Esposito et al., 2006) and included the posterior cingulate cortex (PCC), extending dorsally into the pre-cuneus along the midline, the inferior parietal cortex (IPC), organized in bilateral spots at the occipito-parietal junction, and the medial pre-frontal cortex (MPFC), that included the perigenual part of the anterior cingulate cortex (ACC). In addition, two functional clusters were co-activated to this network, encompassing bilaterally the hippocampus. Fig. 1 (a, b, c) shows the 3d rendering of all DMN volumes of activity respectively for 0-, 1- and 2-back task modulation. The overall DMN extension (as quantified by the total volume of activity at the selected threshold) increased with task difficulty from 0.104178 liters in the 0-back, to 0.106631 liters in the 1-back (+2.355%) and to 0.110303 liters (+5.88%). The averaged regional time-courses from

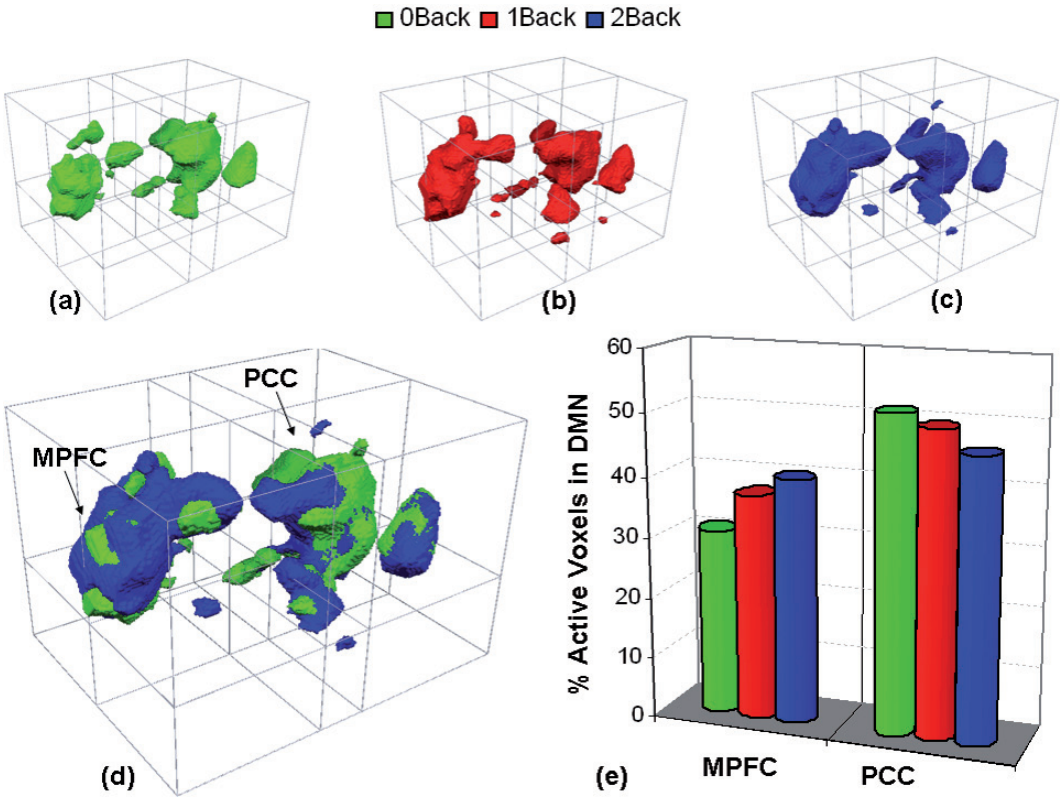

Fig. 1. - Three-dimensional views and comparison of group-level DM component volumes of activity after threshold (z = 3.1, p = 0.001). (a) 0-back (green). (b) 1-back (red). (c) 2-back (blue). (d) Superposition of 0-back (green) and 2-back (blue). (e) Relative percent of active voxels in MPFC and PCC volumes with respect to the entire activity within the default-mode component.

the overall group-level DMN (i.e. all regions of activity combined) were negatively and parametrically correlated with the stimulus function (-0.1671 in the 0-back, -0.4303 in the 1-back and -0.5011), reflecting the expected load-dependent deactivation elicited by the N-back task in the DMN regions (see also Esposito et al., 2006).

A variable recruitment of the cingulate regions across n-back sessions with greater extension of the anterior and lesser extension of the posterior cingulate regions when moving from lower to higher working memory loads was observed. Fig. 1d shows the superposition of DMN volumes of activity for the 0-back (green) and 2-back (blue) and allows visualizing anteriorly the relative prevalence of MPFC activity during the 2-back task (the blue cluster surface mostly encloses the green cluster surface) and posteriorly the relative prevalence of PCC activity during the 0-back task (the green cluster surface mostly encloses the blue cluster surface). This prevalence (and the corresponding modulation from 0- to 1- and 2-back) is also visible in the bar graph of Fig. 1e where the percentage ratios of active voxels in MPFC and PCC volumes relative to the entire DMN volume of activity in the group-level DMN map are descriptively reported for all n-back sessions.

Starting from the group-level DMN component maps (and specifically from the random effects maps thresholded at $z = 3.1$, $p = 0.001$), the MPFC and PCC volumes were identified, quantified and compared to the homologous regions for the different cognitive loads in each single subject/session DMN component. The percentage ratios of active voxels inside the MPFC and PCC to the total number of active voxels in the entire individual DMN component were calculated for all sessions and subjects and correlated with the three levels of task difficulty and the individual performances in an ANCOVA analysis. Although the group-level DMN maps were only used to identify and tag the MPFC and PCC spots in the single-subject DMN maps, we explicitly verified that the observed difference in the extension of the VOIs in the group-level maps across the three sessions did not affect the calculated percentage ratios of active voxels.

Fig. 2 reports the outcome of the ANCOVA for the two regions of interest, PCC (Fig. 2a) and MPFC (Fig. 2b). In Fig. 2, both the scatter plots of the repeated measurements versus the task performances are reported for each separate level of task difficulty together with the linear trend line and the ANOVA tables quantifying the statistical significance of the two factors task difficulty ("N-back") and task performance ("Performance"). Although the observed dispersion of the performances across the subjects of our sample was high only for the 2-back sessions (0- and 1-back performances from all subjects were all very close to 100% of accuracy), both factors were found to be statistically significant ($p < 0.0001$ for the task difficulty and $p = 0.0017$ for the task performance). No significant interaction was found between the two factors. Considering the 2-back sessions only, we found a statistically significant positive correlation for the MPFC ($R^2 = 0.4147$, $p = 0.0022$) and a statistically significant negative correlation for the PCC ($R^2 = 0.2216$, $p = 0.0362$).

Discussion

We have presented ICA results from three different sessions of the working memory experiment based on the n-back task. The cognitive load varied from 0-back to 2-back in three different sessions where the subjects alternated between periods of rest and period of task performance. Our attention was focused on the DMN independent component which was characterized by a substantially load-invariant global layout, with a systematic functional coupling between MPFC, PCC and the other known DMN regions, and a parametric load-dependent functional deactivation. A parametric increase in the overall volume of DMN functional connectivity was also observed which can be explained by the fact that increasing levels of local deactivation necessarily contribute the increased levels of overall distributed correlations.

Within these distributed patterns, the two cingulate spots were significantly modulated in their volumetric extent by the varying cognitive engagement implied by the working-memory task. Although descriptive and exploratory in its nature, this finding was consistent with our previous work (Esposito et al., 2006).

As a major advancement with regards to the previous literature on the modulation of the cingulate network by the cognitive load, the relative extents of MPFC and PCC volumes significantly correlate

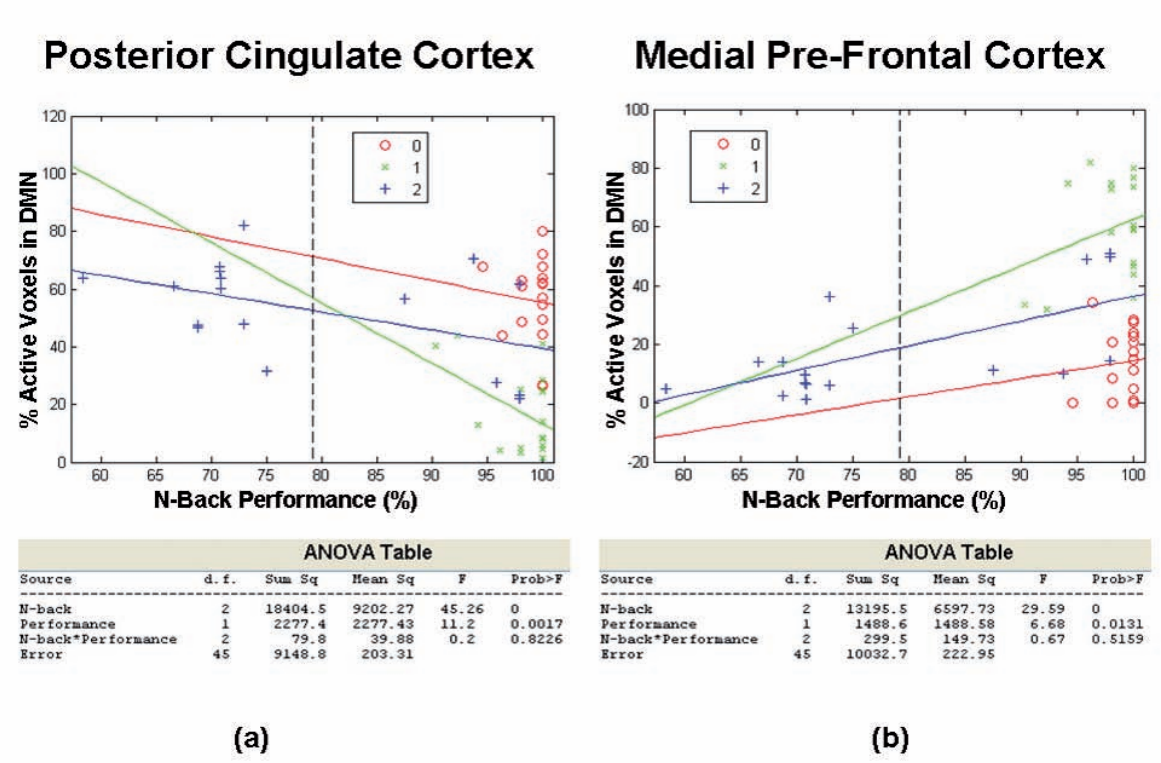

Fig. 2. - Analysis of covariance (ANCOVA) of the individual percentages of relative DMN connectivity in PCC (a) and MPFC (b) with the task difficulty and performances as factors. The scatter plots for the comparison of individual volumes of relative DMN activity in PCC (a) and MPFC (b) with N-back performances are shown in the upper parts of the figure (0-, 1- and 2-back dispersions and correlations are shown in different colors). In each graph, the linear trend fit lines are also plotted. The ANOVA tables expressing the statistical significance of the task difficulty (N-Back) and task performance (Performances) factors are displayed in the lower parts of the figure.

with the average accuracy in the working-memory task at the 2-back level of difficulty. In order to produce such evidence, we took advantage of a rather large number of subjects (n = 17) and the resulting substantial variability in the individual performances, thereby making possible to evaluate the linear correlation between the spatial distribution of the individual DMN components and the corresponding individual working-memory performances, as quantified by the average accuracy in the n-back task.

Although the necessary statistical significance in the linear correlation tests was achieved only for the 2-back task, where the difficulty was high enough to produce enough variability in the performances, we could basically demonstrate that the relative involvement of MPFC and PCC inside the DMN network represents not only a reproducible effect of the memory requirement but also a correlate of the average accuracy in the memory performance.

The dependence of MPFC and PCC extents with task difficulty reflects a spatial re-distribution or re-organization of the functional connectivity within and between the main DMN regions and can be seen as a possible physiological response of the default-mode system to the increasing cognitive engagement of the subject. More specifically, increasing cognitive loads shift the recruitment of cingulate cortex neurons to the DMN functional connectivity pattern from more posterior (PCC) to more anterior (MPFC) populations, and the more manifest (and efficient) this mechanism the better the accuracy in the task. Therefore, we can speculate that this mechanism is also the physiological response to the increasing need of focused attention and task-unrelated thought suppression implied by the increasing task difficulty.

The correlation of default-mode region activity with task performances has been previously inter-

preted in relation to either a specific cognitive deficit (Weinberger et al., 1996; Callicott et al., 1998; Aleman et al., 1999; Bertolino et al., 2004; Gazzaley et al., 2005) or to the different general attention status of the subjects and the engagement in unrelated thought activities interfering with stimulus processing (Fransson, 2006; Golland et al., 2007; Mason et al., 2007). Given that our study only included healthy volunteer subjects, higher or lower skills in carrying out the 2-back task can be related to physiological factors inherent to the mental processing of the stimulus. Following this line, the observed variability of functional connectivity might parallel the amount of interference existing between task-unrelated and task-related processing (Fransson, 2006): higher or lower skills in carrying out the cognitive task would thus become linked directly to the ability of the subject of fruitfully balancing between internal processing (i.e. keeping an old item memorized) and external processing (i.e. acquiring a new item).

As a secondary finding of this study, the variable involvement of the cingulate regions (MPFC and PCC) across the n-back sessions with greater extent of the anterior and lesser extension of the posterior clusters at increasing cognitive loads fully replicates previous study (Esposito et al., 2006), extending substantially, with regard to this study, the number of subjects for the group-level analysis.

The link existing between the extent of the main DMN regions and the performance in a working-memory task suggests that the PCC and MPFC have a main role in focused attention and working memory processes (Fox et al., 2005). In the study by Fox et al. (2005), the functional connectivity of the task-negative (DMN) regions has been directly put in connection with the functional connectivity of the task-positive regions during focused attention and working memory via a 2-network model based on two anti-correlated networks. According to this model, task-negative (DMN) regions are anti-correlated with task-positive regions not only during the performance of a cognitive task but also during continuous periods of fixation. With respect to this point, it is important here to note that the 2-network model of anti-correlated regions appears not to fully explain the variance (and covariance) typically measured with whole-brain fMRI time series, nor is able to characterize the DMN system in all possible experimental scenarios. In fact, a perfect and systematic negative correlation between the two separate sets of regions would cause ICA keeping all regions from the two networks inside the same network, rather than separating them in two or more spatially independent components. According to the ICA model (which is region and task independent), the DMN regions appear to be systematically correlated (and, thus, functionally connected) with each other, while the anti-correlation of these regions with other task-positive regions is at least not systematic during the entire period of observation.

In conclusion, accepting the exploratory flavour of the presented results, we suggest that the efficiency of the working-memory function might be linked to the balanced modulation of the cingulate regions within the distributed pattern of functional connectivity characterizing the DMN network, as extracted by spatial ICA. Accurate cognitive performances are probably facilitated by the spatial re-distribution of functional connectivity between a more extended deactivation in MPFC and a less extended deactivation in PCC regions and this mechanism appears fully consistent with the so-far postulated functional role of the DMN system consisting in regulating focused attention and task-unrelated thought suppression for better monitoring of the cognitive performance.

References

Aleman A., Hijman R., de Haan E.H.F., Kahn R.S. Memory Impairment in Schizophrenia: A Meta-Analysis. *Am. J. Psychiatry*, **156**: 1358-1366, 1999.

Bartels A. and Zeki S. Brain dynamics during natural viewing conditions - a new guide for mapping connectivity in vivo. *Neuroimage*, **24** (2): 339-349, 2005.

Baumgartner R., Windischberger C., Moser E. Quantification in functional magnetic resonance imaging: fuzzy clustering vs. correlation analysis. *Magn. Reson. Imaging*, **16** (2): 115-125, 1998.

Bertolino A., Caforio G., Blasi G., De Candia M., Latorre V., Petruzzella V., Altamura M., Nappi G., Papa S., Callicott J.H., Mattay V.S., Bellomo A., Scarabino T., Weinberger D.R., Nardini M. Interaction of COMT Val108/158 Met Genotype and Olanzapine Treatment on Prefrontal Cortical Function in Patients With Schizophrenia. *Am. J. Psychiatry*, **161** (10): 1798-1805, 2004.

Biswal B., Yetkin F.Z., Haughton V.M., Hyde J.S. Functional connectivity in the motor cortex of resting human brain using echo-planar MRI. *Magn. Reson. Med.*, **34** (4): 537-541, 1995.

Biswal B.B., Van Kylen J., Hyde J.S. Simultaneous assessment of flow and BOLD signals in resting-state functional connectivity maps. *NMR Biomed.*, **10** (4-5): 165-170, 1997.

Calhoun V.D., Adali T., Pearlson G.D., Pekar J.J. Spatial and temporal independent component analysis of functional MRI data containing a pair of task-related waveforms. *Hum. Brain Mapp.*, **13** (1): 43-53, 2001.

Bonino D., Ricciardi E., Sani L., Gentili C., Vanello N., Guazzelli M., Vecchi T., Pietrini P. Tactile spatial working memory activates the dorsal extrastriate cortical pathway in congenitally blind individuals. *Arch. Ital. Biol.*, **146** (3-4): 133-146, 2008.

Callicott J.H., Ramsey N.F., Tallent K., Bertolino A., Knable M.B., Coppola R., Goldberg T., van Gelderen P., Mattay V.S., Frank J.A., Moonen C.T., Weinberger D.R. Functional magnetic resonance imaging brain mapping in psychiatry: methodological issues illustrated in a study of working memory in schizophrenia. *Neuropsychoph.*, **18** (3): 186-196, 1998.

Ciesielski K.T., Lesnik P.G., Savoy R.L., Grant E.P., Ahlfors S.P. Developmental neural networks in children performing a Categorical N-Back Task. *Neuroimage*, **33** (3): 980-990, 2006.

Cordes D., Haughton V.M., Arfanakis K., Wendt G.J., Turski P.A., Moritz C.H., Quigley M.A., Meyerand M.E. Mapping functionally related regions of brain with functional connectivity MR imaging. *AJNR Am. J. Neuroradiol.*, **21** (9): 1636-1644, 2000.

Damoiseaux J.S., Beckmann C.F., Arigita E.J., Barkhof F., Scheltens P., Stam C.J., Smith S.M., Rombouts S.A. Reduced resting-state brain activity in the "default network" in normal aging. *Cereb. Cortex*, **18** (8): 1856-1864, 2008.

Damoiseaux J.S., Rombouts S.A., Barkhof F., Scheltens P., Stam C.J., Smith S.M., Beckmann C.F. Consistent resting-state networks across healthy subjects. *Proc. Natl. Acad. Sci. U S A.*, **103** (37): 13848-13853, 2006.

Esposito F., Aragri A., Pesaresi I., Cirillo S., Tedeschi G., Marciano E., Goebel R., Di Salle F. Independent component model of the default-mode brain function: combining individual-level and population-level analyses in resting-state fMRI. *Magn. Reson. Imaging*, **26** (7): 905-913, 2008.

Esposito F., Bertolino A., Scarabino T., Latorre V., Blasi G., Popolizio T., Tedeschi G., Cirillo S., Goebel R., Di Salle F. Independent component model of the default-mode brain function: Assessing the impact of active thinking. *Brain Res. Bull.*, **70** (4-6): 263-269, 2006.

Esposito F., Scarabino T., Hyvarinen A., Himberg J., Formisano E., Comani S., Tedeschi G., Goebel R., Seifritz E., Di Salle F. Independent component analysis of fMRI group studies by self-organizing clustering. *Neuroimage*, **25** (1): 193-205, 2005.

Fox M.D., Snyder A.Z., Vincent J.L., Corbetta M., Van Essen D.C., Raichle M.E. The human brain is intrinsically organized into dynamic, anticorrelated functional networks. *Proc. Natl. Acad. Sci. U S A*, **102** (27): 9673-9678, 2005.

Fransson P. How default is the default mode of brain function? Further evidence from intrinsic BOLD signal fluctuations. *Neuropsychologia*, **44** (14): 2836-2845, 2006.

Friston K.J., Fletcher P., Josephs O., Holmes A., Rugg M.D., Turner R. Event-related fMRI: characterizing differential responses. *Neuroimage*, **7** (1): 30-40, 1998.

Gazzaley A., Cooney J.W., Rissman J., D'Esposito M. Top-down suppression deficit underlies working memory impairment in normal aging. *Nat. Neurosci.*, **8** (10): 1298-1300, 2005.

Gevins A. and Cutillo B. Spatiotemporal dynamics of component processes in human working memory. *Electroencephalogr. Clin. Neurophysiol.*, **87** (3): 128-143, 1993.

Goldman-Rakic P.S. Working memory dysfunction in schizophrenia. *J. Neuropsychiatry Clin. Neurosci.*, **6** (4): 348-357, 1994.

Golland Y., Bentin S., Gelbard H., Benjamini Y., Heller R., Nir Y., Hasson U., Malach R. Extrinsic and intrinsic systems in the posterior cortex of the human brain revealed during natural sensory stimulation. *Cereb. Cortex*, **17** (4): 766-777, 2007.

Goutte C., Toft P., Rostrup E., Nielsen F., Hansen L.K. On clustering fMRI time series. *Neuroimage*, **9** (3): 298-310, 1999.

Greicius M.D., Krasnow B., Reiss A.L., Menon V. Functional connectivity in the resting brain: a network analysis of the default mode hypothesis. *Proc. Natl. Acad. Sci. U S A*, **100** (1): 253-258, 2003.

Greicius M.D. and Menon V. Default-mode activity during a passive sensory task: uncoupled from deactivation but impacting activation. *J. Cogn. Neurosci.*, **16** (9): 1484-1492, 2004a.

Greicius M.D., Srivastava G., Reiss A.L., Menon V. Default-mode network activity distinguishes Alzheimer's disease from healthy aging: evidence from functional MRI. *Proc. Natl. Acad. Sci. U S A*, **101** (13): 4637-4642, 2004b.

Hampson M., Driesen N.R., Skudlarski P., Gore J.C., Constable R.T. Brain connectivity related to working memory performance. *J. Neurosci.*, **26** (51): 13338-13343, 2006.

Himberg J., Hyvarinen A., Esposito F. Validating the independent components of neuroimaging time series via clustering and visualization. *Neuroimage*, **22**: 1214-1222, 2004.

Hyvarinen A., Karhunen J., Oja E. *Independent Component Analysis*. John Wiley & Sons, Inc., New York, Chichester, Weinheim, Brisbane, Singapore, Toronto, 2001.

Jansma J.M., Ramsey N.F., Coppola R., Kahn R.S. Specific versus nonspecific brain activity in a parametric n-back task. *Neuroimage*, **12** (6): 688-697, 2000.

Mason M.F., Norton M.I., Van Horn J.D., Wegner D.M., Grafton S.T., Macrae C.N. Wandering minds: the default network and stimulus-independent thought. *Science*, **315** (5810): 393-395, 2007.

Mazoyer B., Zago L., Mellet E., Bricogne S., Etard O., Houdé O., Crivello F., Joliot M., Petit L., Tzourio-Mazoyer N. Cortical networks for working memory and executive functions sustain the conscious resting state in man. *Brain. Res. Bull.*, **54** (3): 287-298, 2001.

McKeown M.J., Hansen L.K., Sejnowsk T.J. Independent component analysis of functional MRI: what is signal and what is noise? *Curr. Opin. Neurobiol.*, **13** (5): 620-629, 2003.

McKiernan K.A., Kaufman J.N., Kucera-Thompson J., Binder J.R. A parametric manipulation of factors affecting task-induced deactivation in functional neuroimaging. *J. Cogn. Neurosci.*, **15**: 394-408, 2003.

Morcom A.M., Fletcher P.C. Does the brain have a baseline? Why we should be resisting a rest. *Neuroimage*, **37** (4): 1073-1082, 2007.

Owen A.M., McMillan K.M., Laird A.R., Bullmore E. N-back working memory paradigm: a meta-analysis of normative functional neuroimaging studies. *Hum. Brain Mapp.*, **25** (1): 46-59, 2005.

Pecini C., Biagi L., Guzzetta A., Montanaro D., Brizzolara D., Cipriani P., Chilosi A., Tosetti M., Cioni G. Brain representation of phonological processing in Italian: individual variability and behavioural correlates. *Arch. Ital. Biol.*, **146** (3-4): 189-203, 2008.

Raichle M.E., MacLeod A.M., Snyder A.Z., Powers W.J., Gusnard D.A., Shulman G.L. A default mode of brain function. *Proc. Natl. Acad. Sci. U S A*, **98** (2): 676-682, 2001.

Raichle M.E., Snyder A.Z. A default mode of brain function: a brief history of an evolving idea. *Neuroimage*, **37** (4): 1083-1090, 2007.

Rombouts S.A., Barkhof F., Goekoop R., Stam C.J., Scheltens P. Altered resting state networks in mild cognitive impairment and mild Alzheimer's disease: an fMRI study. *Hum. Brain Mapp.*, **26** (4): 231-239, 2005a.

Rombouts S.A., Goekoop R., Stam C.J., Barkhof F., Scheltens P. Delayed rather than decreased BOLD response as a marker for early Alzheimer's disease. *Neuroimage*, **26** (4): 1078-1085, 2005b.

Rombouts S.A., Stam C.J., Kuijer J.P., Scheltens P., Barkhof F. Identifying confounds to increase specificity during a "no task condition". Evidence for hippocampal connectivity using fMRI. *Neuroimage*, **20** (2): 1236-1245, 2003.

Sambataro F., Murty V.P., Callicott J.H., Tan H.Y., Das S., Weinberger D.R., Mattay V.S. Age-related alterations in default mode network: Impact on working memory performance. *Neurobiol. Aging*. In press.

Sorg C., Riedl V., Mühlau M., Calhoun V.D., Eichele T., Läer L., Drzezga A., Förstl H., Kurz A., Zimmer C., Wohlschläger A.M. Selective changes of resting-state networks in individuals at risk for Alzheimer's disease. *Proc. Natl. Acad. Sci. U S A*, **104** (47): 18760-18765, 2007.

Talairach J. and Tournoux P. *Co-planar Stereotaxic Atlas of the Human Brain*. George Thieme Verlag Stuttgart, Thieme Medical Publishers, Inc., New York 1988.

van de Ven V.G., Formisano E., Prvulovic D., Roeder C.H., Linden D.E. Functional connectivity as revealed by spatial independent component analysis of fMRI measurements during rest. *Hum. Brain Mapp.*, **22** (3): 165-178, 2004.

Weinberger D.R., Mattay V., Callicott J., Kotrla K., Santha A., van Gelderen P., Duyn J., Moonen C., Frank J. fMRI applications in schizophrenia research. *Neuroimage*, **4**: S118-126, 1996.